TOWARDS A NOVEL DUAL-MODALITY IMAGING USING SCATTERED RADIATION

J. L. Delarbre, M. K. Nguyen

Equipes Traitement des Images et du Signal (ETIS)
CNRS / ENSEA / Université de Cergy-Pontoise
6 avenue du Ponceau,
95014 Cergy-Pontoise Cedex, France

T. T. Truong

Laboratoire de Physique Théorique et Modélisation (LPTM)
CNRS / Université de Cergy-Pontoise
2 rue Adolphe Chauvin,
95032 Cergy-Pontoise Cedex, France

ABSTRACT

This paper presents a new dual-modality imaging principle using two recent results. The first one demonstrates the feasibility of reconstruction of a radioactive distribution from its Compton-scattered radiation. This may be regarded as a novel gamma-ray emission imaging principle. The second one shows the possibility to reconstruct the electronic density of a medium and its attenuation map from other Compton-scattered radiation emitted by an external gamma source and scattered in the medium. The required data for the two reconstructions are easily acquired from an energy and space measuring gamma camera under the form of scattered distribution images classified by their Compton-scattering angle. The usual motion of camera is no longer necessary and so all images needed for a three-dimensional reconstruction are recorded simultaneously. For non-immobile object, this is a decisive advantage.

1. INTRODUCTION

Transmission and emission imaging are two complementary modalities of nuclear imaging. Structural informations of an object are brought out by its matter density and revealed by attenuation of gamma or X radiations in it. This technique shows anatomical structures of the body or industrial defects in a second case. Radioactive substance such as radiopharmaceutical or some industrial fluid could be imaged by its radiation with a gamma or X detector. In this way, functional informations of the body or a system (like fluid flow) are revealed. Particulary for medical applications, dual-modality imaging brings more than the sum of its components [1]. X-ray computed tomography (CT) data are used to generate a patient-specific attenuation map and anatomical data which are used to correct errors due to photon attenuation, scattered radiation and other physical effect in radionuclide data such as single-photon emission computed tomography (SPECT) or positron emission tomography (PET). More over, this information can be interpreted by the diagnostician to detect, localize and diagnose hyperfixations of radionuclide. Since the pioneers of nuclear medicine such Mayneord, Anger, Cameron and Sorenson, it is recognized that a radionuclide imaging system could be augmented by using an external radioisotope source to acquire transmission data for anatomical correlation of the emission image. Nowadays, SPECT/CT and PET/CT dual-modality imaging systems are proposed by the major medical equipment manufacturers for clinical use. Those equipments make dual-modality imaging easier because of patient motion limitation and quasi simultaneity of acquisition. In despite of those improvement, many challenges still occur. X-ray process is far shorter than scintigraphic one, so images does not superposable exactly. Scattered radiations of radionuclide disturb CT data, and contrast product damages radionuclide data.

In the present work, we present two alternative approches by taking advantage of the properties of scattered photons and we show that these photons can be used to improve the image quality. In section 2, by modeling the Compton diffusion we introduced the so-called compounded conical Radon transform (CCRT) [2] [3] [4], which is considered as a generalization of the classical Radon transform. The invertibility of the CCRT demonstrates the feasibility of reconstruction of an three dimensional (3D) object from a series of images indexed by the angle of scattering (or equivalently by the outgoing energy). The quality of the reconstruction object shows the relevance of the CCRT in modeling the scattered radiation and the efficience of the reconstruction algorithm. In section 3, a new method is proposed to obtain the attenuation map and so structural informations of a medium via the determination of its electron density using the Compton effect and subsequent algorithm steps. The methods consists in determining first the electron density without taking care of attenuation and just exploiting the properties of the Compton effect. Then the corresponding attenuation coefficients are computed and serve as a first approximation and which should be used next in a following determination of the electron density. Thus an iterative procedure is set up with a specialized algorithm in order to arrive at final form of the attenuation (or structural) map.

2. SCATTERED GAMMA-RAY EMISSION IMAGING

The point of view adopted in this work, is to focus on the emitted photons which undergo at least one Compton scattering at various levels and to study how they may turn out to be relevant for three dimensional reconstruction process of a gamma source. Fig. 1 illustrates our calculations.

Let $\mathbf{V}$ denote an object voxel of coordinates (ξ_V, η_V, ζ_V) and $f(\mathbf{V})$ be the object activity density function, defined as $f(\mathbf{V}) = f(\xi_V, \eta_V, \zeta_V)$. This is also the number of photons emitted per unit time and per unit object (or source) volume, uniformly distributed in space at site $\mathbf{V}$. Thus, we have the number of photons receved at $\mathbf{M}$ equals to:

$$\frac{1}{4\pi\, MV^2} f(\mathbf{V}) d\mathbf{V}. \tag{1}$$

If there is a Compton collision at site $\mathbf{M}$ with the electron density in medium n_e, the number of photons reaching a unit detector surface at $\mathbf{D}$ per unit time is the flux density recorded by the detector at site $\mathbf{D}$:

$$\frac{f(\mathbf{V})d\mathbf{V}}{4\pi\, MV^2}\, n_e\, d\mathbf{M}\, \frac{r_e^2}{2}\, P(\theta)\, \frac{1}{MD^2}, \tag{2}$$

where r_e is the classical radius of the electron and $P(\theta)$ the so-called

Klein-Nishina probability for deflection by an angle θ. The absorption is neglected here.

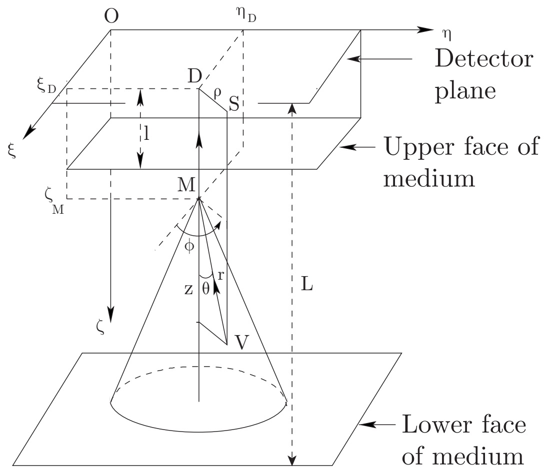

Fig. 1. Coordinate system for the calculation of CCRT

Consequently, the number of photons recorded per unit time and unit detector area at site $\mathbf{D} = (\xi_D, \eta_D)$, $\tilde{g}(\mathbf{D}, \theta)$, is due to all emitting point sources $\mathbf{V}$ situated on a cone with opening angle θ, axis parallel to $O\zeta$ and with apex the scattering site on the vertical line MD:

$$\tilde{g}(\mathbf{D}, \theta) = \int d\xi_M d\eta_M \frac{d\zeta_M}{\zeta_M^2} \delta(\xi_D - \xi_M)\delta(\eta_D - \eta_M) n_e$$

$$\int \frac{f(\mathbf{V}) d\mathbf{V}}{4\pi} \frac{\delta(Cone)}{MV^2} \frac{r_e^2}{2} P(\theta), \tag{3}$$

where $\delta(Cone)$ restricts the integration over $\mathbf{V}$ to the circular cone. If one uses the local spherical coordinates centered at $\mathbf{M}$ in Fig. 1, we have $d\mathbf{V} = r^2 dr \sin\alpha d\alpha d\phi$ then $\delta(Cone) = \frac{1}{r}\delta(\theta - \alpha)$.

We can rewrite this transformation in a more suggestive form using $t = \tan\theta$, $\tilde{K}(\theta) = K(t)$ and $\tilde{g}(\mathbf{D}, \theta) = g(\mathbf{D}, t)$, as:

$$g(\mathbf{D}, t) = \int d\mathbf{V}\, p(\mathbf{D}, t|\mathbf{V})\, f(\mathbf{V}). \tag{4}$$

where $p(\mathbf{D}, t|\mathbf{V})$ stands for the kernel of the transformation, which will be called compounded conical Radon transform (CCRT) from now on.

Physically this kernel is also called the Point Spread Function (PSF), or image of a point source at site $\mathbf{V} = (\xi, \eta, \zeta)$. The mathematical computation of the PSF kernel leads to the following expression:

$$p(\mathbf{D}, t|\mathbf{V}) = Y(t) t^2 K(t) \frac{Y(t(\zeta - l) - \rho)}{\rho^2 (t\zeta - \rho)^2}$$

$$+ Y(-t) t^2 K(t) \frac{1}{\rho^2 (|t|\zeta + \rho)^2}, \tag{5}$$

valid in the whole range of t values. $Y(...)$ is the Heaviside unit step function, and

$$\tilde{K}(\theta) = \frac{n_e}{4\pi} \frac{r_e^2}{2} P(\theta) \sin\theta \tag{6}$$

We have shown that the transformation CCRT is *invertible* [3]. This is the foundation of the new tree dimensional object reconstruction.

$$F(u, v, w) = \frac{1}{\mathcal{J}_l^L(w)} \int dz\, e^{2\imath\pi z w} [-|z|\sqrt{u^2 + v^2}]\, e^{2\imath\pi l w}$$

$$\int_0^\infty t\, dt J_1(2\pi |z| t \sqrt{u^2 + v^2})$$

$$\{Y(z) \frac{\partial}{\partial t} \frac{G(u, v, t)}{K(t)} + Y(-z) \frac{\partial}{\partial t} \frac{G(u, v, -t)}{K(-t)}\} \tag{7}$$

The tree-dimensional Fourier transform of $f : F$ is expressed as a transform of the bidimensional Fourier transform of $g : G$, where $J_1(.)$ is the first order Bessel function and

$$\mathcal{J}_l^L(w) = \frac{e^{2\imath\pi l w}}{l} - \frac{e^{2\imath\pi L w}}{L} + 2\imath\pi w\, [Ei(2\imath\pi L w) - Ei(2\imath\pi l w)] \tag{8}$$

where $Ei(.)$ is the function "exponential integral".

Finally the object activity density $f(V)$ may be recovered by inverse 3D Fourier transform from eq. (7).

We note that no motion of the detector occurs during the recording process of data and all view necessary for a 3D reconstruction are record simultaneously.

3. SCATTERED GAMMA-RAY TRANSMISSION IMAGING

In this section we demonstrate how to reconstruct the electron density of a medium (n_e) to obtain its internal structure and subsequently its attenuation map. The novelty of the method consists in collecting the scattered photons on a fixed planar detector in order to determine n_e, (as opposed to moving source and point detector in the Compton scatter imaging method). Usually scattered radiation is considered to be a nuisance and has to be discarded. But here they are collected and provide information on the electron density.

3.1. Image formation and electron density reconstruction formulas

Neglecting first attenuation and multiple scattering, we establish a formula giving the measured photon flux density at a detector site in terms of the external source intensity and the electron density of medium under study. Fig. 2 illustrates this working principle.

At given scattering angle θ (or at given outgoing photon energy), the recorded photon flux density on the detector is proportional to the electron density and source intensity f_0:

$$g(\mathbf{D}, \theta) = n_e(\mathbf{M}) \frac{f_0\, r_e^2}{8\pi} \frac{1}{\zeta_M^2} \frac{\sin^2\theta}{\rho^2} P(\theta) \tag{9}$$

where $\rho = DS$ and $\zeta_M = DM$.

It is well known that after a Compton scattering event a photon loses a definite part of its energy which is determined by its scattering angle θ. $P(\theta)$ is the Klein-Nishina probability.

One sees that for given scattering site $\mathbf{D}$ and scattering angle θ, there is only one scattering point $\mathbf{M}$, defined by ζ_M. So each measurement on the detector yields a value of the electronic density n_e (see eq. (10)):

$$n_e(\mathbf{M}) = g(\mathbf{D}, \theta) \frac{8\pi\, \zeta_M^2\, \rho^2}{f_0\, r_e^2\, P(\theta) \sin^2\theta} \tag{10}$$

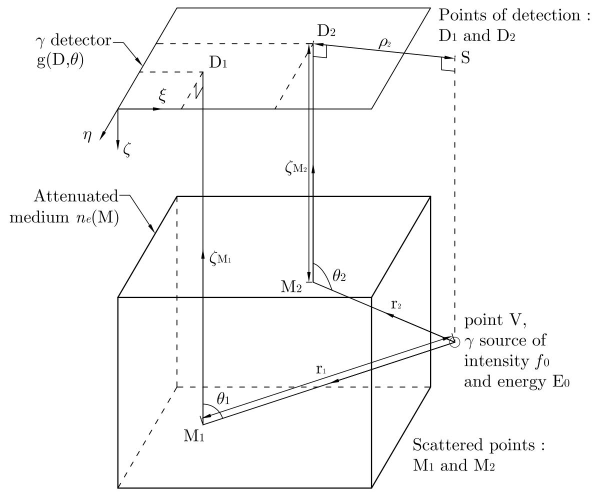

Fig. 2. Geometric parameters of the photon scattering due to a point source

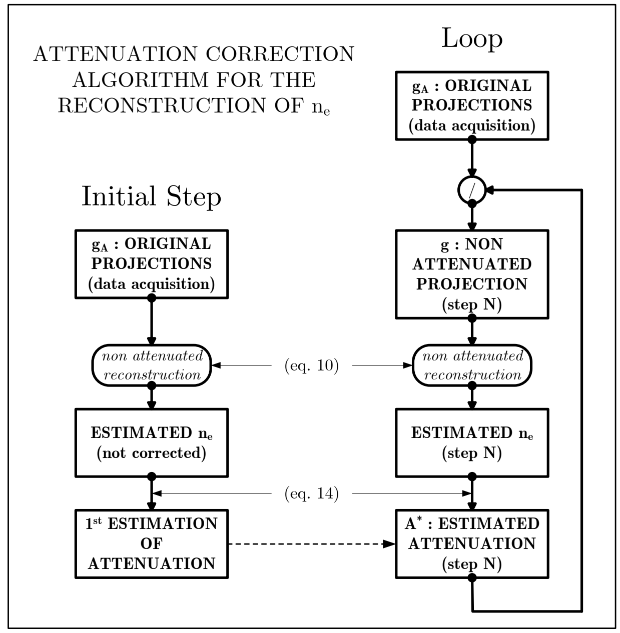

Fig. 3. ISDC algorithm

In the absence of attenuation, this result is mathematically exact. In the next subsection, we will show how attenuation can be accurately obtained through the medium.

3.2. Correction of attenuation in reconstruction of n_e, description of the ISDC algorithm

We describe here the algorithmic steps which yield the successive approximate values of the attenuation map through the respective values of n_e computed as shown in the previous subsection. In this work, we consider radiation with energy range from 50 keV to 150 keV (like ^{99m}Tc) where attenuation is only due to Compton attenuation.

We use the so-called Iterative Scattered Data Correction (ISDC) method to perform attenuation correction and improve the accuracy of the reconstructed electron density. Fig. 3 recalls the principle of this method. The initial step of the algorithm consists of obtain a first estimation of n_e (computed with the reconstruction method formula (10)) and so of the attenuation which will serve next to correct camera images.

Now we always do the same process in the loop with data acquisition. A correction is applied on images recorded by the detector. From those new images, we reconstruct the electron density again with the method formula (10) without attenuation. This last estimation of n_e gives us a new estimation of the attenuation which will be used on the next step. The whole process is summarized in fig. 3.

We have to explain how we exactly do the correction on detector images on each step. The exact expression of the recorded photon flux density is:

$$g_A(\mathbf{D},\theta) = n_e(\mathbf{M})\, A(\mathbf{D},\mathbf{M}) \quad \frac{f_0\, r_e^2}{8\pi}\, \frac{1}{\zeta_M^2}\, \frac{\sin^2\theta}{\rho^2}\, P(\theta) \qquad (11)$$

where $A(\mathbf{D},\mathbf{M})$ is the total attenuation of photons emitted by the source, scattered on $\mathbf{M}$ and detected on $\mathbf{D}$. Its expression is:

$$A(\mathbf{D},\mathbf{M}) = e^{-\int_{S_{in}}^{\mathbf{M}} \mu_{E_0}(s_1)\, ds_1}\, e^{-\int_{\mathbf{M}}^{S_{out}} \mu_{E_\theta}(s_2)\, ds_2} \qquad (12)$$

S_{in} and S_{out} are the incoming and outgoing points of rays in the medium, μ_{E_0} and μ_{E_θ} are linear attenuation coefficient for gamma-rays of energy E_0 and E_θ. So, to be exact eq. (10) have to be transformed in:

$$n_e(\mathbf{M}) = \frac{g_A(\mathbf{D},\theta)}{A(\mathbf{D},\mathbf{M})}\, \frac{8\pi\, \zeta_M^2\, \rho^2}{f_0\, r_e^2\, P(\theta) \sin^2\theta} \qquad (13)$$

but $A(\mathbf{D},\mathbf{M})$ is unknown.

The correction we apply on each step on detector images for each incident photon energy (or scattering angle) is to divide the measured photon flux intensity of a pixel by the estimated attenuation $A^*(\mathbf{D},\mathbf{M})$ of photons for that point. To calculate $A^*(\mathbf{D},\mathbf{M})$, we use the same equation of $A(\mathbf{D},\mathbf{M})$ (eq. (12)). We just have to replace μ_E by μ_E^*, the estimated linear attenuation coefficient.

The next step is to develop an algorithm which will lead to the attenuation map. In the ISDC algorithm, we simulate the scattering of radiation from a point source with nonhomogeneous attenuation. At each iteration step an approximation of μ_E is constructed with the electron density obtained in the previous step. This new value of μ_E will serve to get the next value of n_e. In an elementary volume, eq. (14) gives the relation between these two quantities, where m labels the substance used:

$$\mu_{E,m} = \sigma_{E,m}\, n_e \qquad (14)$$

The scattering cross section $\sigma_{E,m}$ depends on the energy E of the radiation and average atomic number of the substance. This atomic number is however not directly accessible. But we know that the only materials we find in body are soft tissue (water), bone and lungs. For all those materials Z is known.

It is an accepted fact that soft tissue is structurally close to water and its electronic density may vary but will never come close of that of bone or air (e.g. in lungs). Similar considerations, as we made for tissue, are true for bone or lungs. So taking into account the estimated value of n_e, allow to guess what type of material is meet on the study point. Knowing which material exist at the point of interest, we have also Z and so $\sigma_{E,m}$.

After the last iteration, we have obtained the best possible reconstruction of the electron density in the medium. We note that no motion of the detector occurs during the recording process of data and all view necessary for a 3D reconstruction are recorded simultaneously.

4. A NEW DUAL-MODALITY IMAGING USING SCATTERED RADIATION

In the two previous sections, we have presented two novel modalities of gamma imaging (emission and transmission) using scattered radiations. We describe here the way to use the two methods together to get the best of them.

In our work, the external source using for the transmission examination is similar to the injected radionuclide and so conversion of Hounsfield coefficients is not necessary. The first step is the acquisition of transmission data with the punctual source placed near the body of patient. Scattered radiations are recorded by the detector in a fixed position to estimate the specific attenuation map of the patient and their anatomical structures. Then after removing the external source, injection of radiopharmaceutical is administered for the emission examination. Nothing needs to move between the two steps, the patient stays in the same position on the table and the detector does not move. Only motions of the patient (like breathing) disturb the recalage of transmission and emission images for localisation of hyperfixations.

The estimated specific attenuation map could be use to correct functional informations. In our work, we have adapted methods like generalized Chang method to scattered radiations.

The combination of the two reconstructions produces an augmented image giving anatomical and functional informations for an enhanced diagnostic.

5. SIMULATIONS AND RESULTS

As an illustration of the proposed dual-modality imaging using two novel procedures of emission and transmission scanning of scattered gamma-ray, we present the numerical computations for reconstruction of structural and functional images and their combination (recalage and attenuation correction). Fig. 4 presents a slice of an original medical phantom in the thoracic zone within a small organ placed exactly in the middle fixing a concentration of radiopharmaceutical with different nodules. 3D reconstruction of radionuclide distribution with correction of attenuation and its positioning in the body is shown in fig. 5.

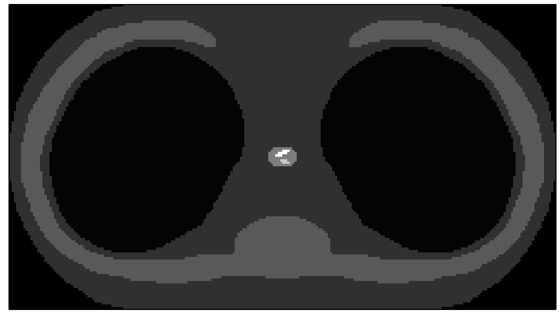

Fig. 4. Original radionuclide distribution and body, the small organ where radionuclide is fixed is placed exactly in the middle

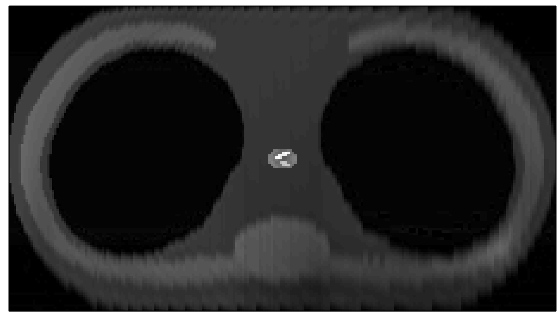

Fig. 5. Reconstructed radionuclide distribution and body

6. CONCLUDING AND REMARKS

In this work, we have shown the principle of a new dual-modality imaging. Structural and functional informations come from scattered radiations. In the first case, an external point source illuminates the object and transmitted and scattered radiations are recorded to reconstruct the medium and its attenuation. These data are useful to scattered gamma-ray emission imaging by allow localization of the radionuclide distribution and correction of attenuation.

The benefits of this new dual-modality imaging is to use only one detector and to take out its motion. Also simpler and less expansive systems are conceivable. Recalage of images is widely simplified, only motion of patient could make some artifacts. Because all views for both emission and transmission are recorded simultaneously (without moving the detector), the time of acquisition could be reduced and temporal coherence of acquisition is preserved.

7. REFERENCES

[1] H. Zaidi, *Quantitative Analysis of Nuclear Medicine Images*, Springer, 2005.

[2] J. L. Delarbre, M. K. Nguyen, T. T. Truong, and J. L. Starck, "Modeling and simulation for scattered gamma-ray imaging," in *Proc. 5th EUROSIM Congress on Modelling and Simulation*, Marne la Valle, France, September 2004, CDROM.

[3] Mai K. Nguyen, T. T. Truong, H. D. Bui, and J. L. Delarbre, "A novel inverse problem in gamma-rays emission imaging," *Inverse Problems in Science and Engineering*, vol. 12, pp. 225–246, 2004.

[4] M. K. Nguyen, T. T. Truong, J. L. Delarbre, and N. Kitanine, "Three-dimensional object reconstruction from compton scattered gamma-ray data," in *Lecture Notes in Computer Sciences*, Milan Sonka, Ioannis Kakadiaris, Jan Kybic, Springer Verlag, and Heildelberg, Eds. 2004, vol. 3117, pp. 24–34, Computer Vision and Mathematical Methods in Medical and Bio-Medical Image Analysis.